Nitric oxide synthase localization in the rat neutrophils: immunocytochemical, molecular, and biochemical studies

R. Saini,* S. Patel,* R. Saluja,* A. A. Sahasrabuddhe,† M. P. Singh,‡ S. Habib,† V. K. Bajpai,§ and M. Dikshit*,[1]

*Cardiovascular Pharmacology Unit, §Electron Microscopy Unit, and †Division of Structural and Molecular Biology, Central Drug Research Institute, Lucknow, India; and ‡Industrial Toxicology Research Centre, Lucknow, India

Abstract: Nitric oxide (NO) modulates diverse functions of polymorphonuclear neutrophils (PMNs), but localization of NO synthase (NOS) and identification of its interacting proteins remain the least defined. The present study discerns subcellular distribution of NOS and caveolin-1, a prominent NOS-interacting protein in rat PMNs. Localization of NOS was explored by confocal and immunogold electron microscopy, and its activity was assessed by L-[^{3}H] arginine and 4,5-diaminofluorescein diacetate (DAF-2DA). Reverse transcriptase-polymerase chain reaction using NOS primers and Western blotting demonstrated the presence of neuronal NOS (nNOS) and inducible NOS (iNOS) in PMNs. Immunocytochemical studies exhibited distribution of nNOS and iNOS in cytoplasm and nucleus, and L-[^{3}H] citrulline formation and DAF fluorescence confirmed NOS activity in both fractions. NOS activity correlated positively with calmodulin concentration in both of the fractions. nNOS and iNOS colocalized with caveolin-1, as evidenced by immunocytochemical and immunoprecipitation studies. The results thus provide first evidence of nNOS and iNOS in the nuclear compartment and suggest NOS interaction with caveolin-1 in rat PMNs. *J. Leukoc. Biol.* 79: 519–528; 2006.

Key Words: *polymorphonuclear leukocytes · nitric oxide synthase · diaminofluorescein diacetate · caveolin-1 · nucleus · subcellular localization*

INTRODUCTION

Nitric oxide (NO) regulates several important functions of polymorphonuclear neutrophils (PMNs), including chemotaxis, adhesion, aggregation, apoptosis, and PMN-mediated bacterial killing or tissue damage [1]. The presence of NO synthase (NOS) in the primary granules of PMNs has implied a pivotal cytotoxic role of NO in combating pathogens [2]. Several studies from our laboratory have also demonstrated NO-mediated modulation of free radical generation from PMNs in various physiological and pathological conditions [3–8].

Although the presence of NO in the subcellular compartments can be of significance in modulating diverse targets, only one study is available about the localization of NOS in intracellular locations by immunohistochemistry [2]. Inducible NOS (iNOS) and constitutive NOS activity and immunoreactivity were associated with various subcellular compartments as well as with the nucleus of endothelial cells [9], brown adipocytes [10], and astrocytes [11]. A recent report about the nuclear localization of biopterin (BH_4) biosynthesizing enzymes, guanosine 5′-triphosphate cyclohydrolase I, 6-pyruvoyl-tetrahydropterin synthase, and sepiapterin reductase is of considerable relevance to the availability of a redox-sensitive cofactor to support NO synthesis in the nuclear compartment [12]. Although biochemical and molecular characteristics of NOS are well explored [5, 13, 14], there is no report available about NOS localization in rat PMNs. Although only neuronal NOS (nNOS) is constitutively expressed in rat PMNs, induction of iNOS has been documented within 2 h after lipopolysaccharide (LPS) treatment [14]. Several splice variants of nNOS have been reported: nNOSα, a full-length protein has a PSD-95/discs large/ZO-1 homology (PDZ) domain, and nNOSβ and nNOSγ lack this domain [15]. Primers used by Greenberg et al. [14] did not verify the presence of PDZ domain in nNOS being expressed in rat PMNs.

Sequestration of NOS in intracellular compartments is a result of various interacting proteins [16], which modulate its enzymatic activity [17–19], spatial distribution [20], proximity with regulators [21, 22], and intended targets [23]. Caveolin-1, a prominent NOS-interactive protein, negatively modulates endothelial NOS (eNOS), nNOS, and iNOS by interfering with calmodulin (CaM) binding [24–26]. The present study was undertaken to investigate the hitherto unexplored subcellular localization of NOS isoforms and caveolin-1 in the rat-circulating PMNs.

MATERIALS AND METHODS

Reagents and antibodies

L-[^{3}H] Arginine and goat anti-mouse and goat anti-rabbit protein A gold were from Amersham Pharmacia Biotech (Uppsala, Sweden). Uranyl acetate was from Polaron Equipment Ltd. (Watford, UK). Monoclonal antibodies (mAb) to

[1] Correspondence: Cardiovascular Pharmacology Unit, Central Drug Research Institute, Lucknow-226001, India. E-mail: madhudikshit@yahoo.com

Received June 15, 2005; revised September 23, 2005; accepted September 29, 2005; doi: 10.1189/jlb.0605320.

nNOS (N-2280) and iNOS (N-9657) and all other chemicals were from Sigma-Aldrich Co. (St. Louis, MO).

Rabbit polyclonal antibodies against caveolin-1 (N-20: sc-894), iNOS (M-19: sc-650G), nNOS (K-20: sc-1025), and horseradish peroxidase goat anti-rabbit/donkey anti-goat were from Santa Cruz Biotechnology (CA). Goat anti-rabbit Oregon Green 488 (OG 488) and anti-mouse indocarbocyanin-5 (Cy5) were from Molecular Probes (Eugene, OR). mAb to rat CD11b-fluorescein isothiocyanate and CD45-phycoerythrin were from BD Biosciences (San Diego, CA).

Animals

Male Sprague-Dawley rats (200–250 g) were obtained from the institute animal house. The animals were kept in a conventional housing facility and were used in accordance with institutional ethical guidelines.

Neutrophil isolation

PMNs were isolated using the method of Yazdanbakhsh et al. [27] with modifications. Buffy coat diluted with phosphate-buffered saline (PBS) containing tri sodium citrate 15 mM, 0.5% (w/v) bovine serum albumin (BSA), and glucose 10 mM was loaded over 1 ml Histopaque-1077 and centrifuged (1000 *g* at 25°C) for 20 min. Original density of cells was restored by suspending cells in rat plasma containing 5% (v/v) fetal calf serum for 30 min. PMNs were separated over Histopaque-1083 and -1119 gradients, washed with PBS, counted, and suspended in Hanks' balanced salt solution [HBSS; composition (mM): NaCl 138, KCl 2.7, Na_2HPO_4 8.1, KH_2PO_4 1.5, glucose 10, pH 7.2–7.4]. PMNs purity was >90% as assessed by CD11b/CD45; contaminating cells in the PMN suspension were mostly lymphocytes.

Isolation of nuclei from PMNs and their morphological characterization

PMNs were fractionated according to Sanghavi et al. [28]. Briefly, cells (1×10^8cells/ml) were suspended in lysis buffer [composition (mM): HEPES 10, NaCl 10, $MgCl_2$ 1.5, EDTA 1, dithiothreitol 5, 10% glycerol, and 0.15% Nonidet P-40 (NP-40), pH 7.4]. After brief vortexing and centrifugation (1700 *g* at 4°C for 5 min), supernatant cytoplasmic fraction (CF) was collected. Nuclei fraction (NF) pellet was washed with lysis buffer (without NP-40) and finally suspended in HBSS (equal to CF). Purity of NF was assessed by DNA content [29] and lactate dehydrogenase (LDH) activity [3]. Purity of NF and the morphological characterization of PMNs in buffy coat were identified under transmission electron microscopy (TEM; FEI Philips Tecnai-12). Buffy coat and isolated nuclei were fixed overnight at 25°C with 2% (w/v) paraformaldehyde and 1% (v/v) glutaraldehyde in PBS (pH 7.4). Fixed nuclei impregnated in 4% buffered agarose were cut into smaller pieces using razor blades, washed thoroughly with PBS, post-fixed in buffered 1% osmium tetroxide for 3 h, dehydrated in ascending series of ethanol, and finally, embedded in Epon and Araldite plastic resin [30]. Ultrathin sections (80–100 nm) cut by Ultra Cut ultramicrotome (Leica, Austria) were contrasted with uranyl acetate and lead citrate and examined under TEM at 80 kV.

Assessment of NOS activity

4,5-Diaminofluorescein diacetate (DAF-2DA) fluorescence

Cells (1×0^7/ml) were washed with HBSS, preincubated with NOS inhibitor 3-bromo 7-nitroindazole (7-NI; 1 mM), NOS substrate L-arginine (1 mM), or vehicle for 30 min at 37°C, and subsequently, incubated with DAF-2DA (10 μM) for 5 min. DAF-loaded PMNs were dispensed on 0.01% (w/v) poly-L-lysine-coated coverslips, and NO production was visualized [31] using BioRad Radiance 2100 laser-scanning system equipped with a Nikon Eclipse TE 300 confocal microscope, with a Plan Apo 60×/1.4 nicotinic acid oil immersion objective. Excitation of Cy5, OG 488, and Hoechst 33258 was performed using 637 nm red diode, 488 nm argon ion, and 405 nm blue diode lasers, and emitted light was detected through HQ660 longpass and HQ515/30 and HQ442/45 bandpass filters, respectively. Data were captured with BioRad LaserSharp 2000 Software 5.1, and photographs were processed using Adobe Photoshop software. Cells without DAF-2DA treatment or fixed cells (1 h with 4% paraformaldehyde), incubated with DAF-2DA, were used as negative controls.

L-[^{3}H] citrulline formation

Total NOS activity (in the presence of 1 mM calcium) and calcium-independent activity (in the absence of calcium and in the presence of 1 mM EGTA) were estimated [4] in PMNs (1×10^7cells) CF and NF, incubated in buffer [composition (mM): HEPES 25, NaCl 140, KCl 5.4, $MgCl_2$ 1, $CaCl_2$ 1, 7 μg/ml pepstatin A, 1.5 μg/ml soybean trypsin inhibitor, 5 μg/ml leupeptin, phenylmethylsulfonyl fluoride (PMSF) 0.5 mM, and benzamidine 0.1 mM, pH 7.4] with cofactors [flavin adenine dinucleotide (FAD) 5 μM, flavin mononucleotide (FMN) 25 μM, reduced nicotinamide adenine dinucleotide phosphate (NADPH) 1 mM, BH_4 10 μM, and 10 μg/ml CaM], and the L-[^{3}H] arginine (0.16 μM) at 37°C. The reaction was terminated after 30 min by stop buffer [composition (mM): NaCl 118, KCl 4.7, KH_2PO_4 1.18, $NaHCO_3$ 1, EDTA 4, N^{ω}-nitro-L-arginine methyl ester 1, pH 5.5] and was passed through a Dowex 50W-X8 column (100–200 mesh, Na^+ form). L-[^{3}H] Citrulline was collected in the unbound wash fraction, and bound L-[^{3}H] arginine was eluted with 0.5 M ammonium hydroxide to obtain citrulline formed from total arginine added in each tube. To investigate the effect of CaM, NOS activity was estimated in CF and NF in the presence of calcium and 10 or 100 μg/ml CaM.

Flow cytometry

PMNs (2×10^6cells/ml) or nuclei were incubated for 30 min with L-arginine (1 mM), 7-NI (1 mM), or vehicle at 37°C and subsequently, loaded with DAF-2DA (10 μM) for 30 min [7]. NO generation was measured by acquiring 10,000 cells/nuclei from each sample and was analyzed by the Cell Quest program.

Assessment of NOS expression

Reverse transcriptase-polymerase chain reaction (RT-PCR)

Total RNA from PMNs and brain samples was extracted using Trizol reagent (Invitrogen, Carlsbad, CA). RNA (5 μg) was reverse-transcribed with Super-Script II RT (Invitrogen) using oligo(dT) primers, as per the manufacturer's instructions. The cDNA was amplified in separate PCRs for NOS isoforms. The PCR products were analyzed by electrophoresis on a 1.2% agarose gel and visualized with ethidium bromide staining. The primers designed with a Primer Select module of Lasergene (DNAStar Inc., Madison, WI) for nNOS (5′-AACGATCGGCCCTTGGTAGAC-3′; 5′-GGGCGGAGCTTTGTGCGATTTG-3′) amplified a 543-base pair (bp) fragment, iNOS (5′-GGACCACCTCTATCAGGAA-3′; 5′-CCTCATGATAACGTTTCTGGC-3′) amplified a 314-bp fragment, and eNOS (5′-TGCTGCCCGAGATATCTTCAGT-3′; 5′-GGCTGCCTTTTTCCAGTTGTTC-3′) amplified a 356-bp fragment. The amplification reactions for 30 cycles were denaturation, 94°C, 30 s; annealing, 49°C, 60°C, and 65°C, 1 min for nNOS, iNOS, and eNOS, respectively; and extension, 72°C, 1 min. RNA from normal and LPS-treated rat brain samples was used as positive controls.

Western blotting (WB) and immunoprecipitation (IP)

PMNs lysate [composition of lysis buffer (mM): NaCl 100, Tris-HCl 10, EDTA 1, 1 μg/ml aprotinin, 100 μg/ml PMSF, 20 μg/ml pepstatin, and sodium orthovanadate 2 mM, pH 7.4], protein was loaded on 15% (for caveolin-1) or 8% (for NOS) sodium dodecyl sulfate-polyacrylamide gel electrophoresis (SDS-PAGE) and transferred onto a polyvinylidene difluoride membrane. Blocking was done overnight [PBS; composition (mM): NaCl 137, KCl 27, Na_2HPO_4 32, K_2HPO_4 15, KH_2PO_4 15, pH 7.4, containing 5% (w/v) BSA], and antibody incubation was for 3 h with polyclonal caveolin-1 and NOS antibodies [1:1000 diluted in PBS containing 0.1% (v/v) Tween-20 and 1% (w/v) BSA]. The specific bands were detected by enhanced chemiluminescence (Sigma-Aldrich Co.), and blots were exposed to the Hyperfilms (Amersham Pharmacia Biotech).

The cells were lysed in radio IP assay buffer [PBS containing 0.1% SDS, 0.5% sodium deoxycholate, 1% Triton X-100, and protease inhibitors (as in lysis buffer)] for 15 min. The supernatant was precleared with protein A/G agarose (Santa Cruz Biotechnology) and incubated with 0.2 μg primary antibody; after 2 h, 20 μl protein A/G agarose was added and incubated for 1 h. The beads were washed, resuspended, and subsequently analyzed by WB. The same concentration of normal immunoglobulin G (IgG) was used in controls for WB and IP.

Confocal microscopy

Subcellular distribution of nNOS, iNOS, and caveolin-1 was examined in fixed PMNs. The cells were fixed in 4% (w/v) paraformaldehyde in PBS (pH 7.4) for

30 min at 25°C and washed two times for 5 min each with PBS containing 0.5% (w/v) glycine. The washed cells were allowed to adhere on 0.01% (w/v) poly-L-lysine-coated coverslips, permeabilized with 0.2% (v/v) Triton X-100 (5–10 min), and blocked with 10% goat serum in PBS for 30 min. Cells were incubated overnight at 4°C with mAb against iNOS/nNOS and polyclonal antibodies against caveolin-1 at a dilution of 1:200 and were subsequently stained at 4°C for 4 h with Cy5 and OG 488-tagged secondary antibodies (1:500), respectively. Nuclei were stained with Hoechst 33258 dye (3 μg/ml) at 25°C for 15 min. Control samples were processed separately by incubating with normal rabbit, mouse, and goat sera or by omitting primary antibodies. Coverslips were mounted in the fluorescence-mounting media (Oncogene, San Diego, CA), and images were acquired as mentioned above. Red, green, and blue images were collected separately with excitations at 647 nm, 488 nm, and 405 nm, respectively, to avoid bleed-through and merged for presentation (Adobe Photoshop software, San Jose, CA).

Immunogold electron microscopy

Buffy coat (obtained by centrifugation of blood at 2000 rpm for 20 min at 25°C) was fixed overnight with 2% (w/v) paraformaldehyde and 0.5% (v/v) glutaraldehyde in PBS (pH 7.4) at 25°C. Small pieces of buffy coat were washed with PBS containing 0.5% (w/v) glycine to quench excess fixative, dehydrated in an ascending series of ethanol, impregnated in London resin-White resin, and subsequently polymerized at 60°C for 48 h. Ultrathin sections (80–100 nm) collected on nickel grids [32] were blocked in PBS containing 0.1% BSA (w/v), 0.1% (v/v) teleost fish gelatin, and 0.05% (v/v) Tween-20 for 30 min and incubated with nNOS or iNOS mAb at 1:500 dilution in blocking buffer for 4 h at 4°C, and subsequently, the sections were incubated with 5/10/15 nm gold-coupled goat anti-mouse IgG (1:20) for 2 h at 37°C and examined under TEM at 80 kV.

In the dual-labeling experiments, ultrathin sections were incubated with polyclonal caveolin-1 antibody (1:500) for 4 h at 4°C and subsequently, with 10 nm gold-coupled goat anti-rabbit IgG (1:20) and then treated with 0.01% glutaraldehyde for 5 min to avoid leaching of gold particles. The excess glutaraldehyde was quenched with 0.5% (w/v) glycine, and sections were incubated with nNOS or iNOS antibodies (1:500) as described above. Sections were washed with blocking buffer and treated with 15 nm gold-coupled anti-mouse IgG antibody (1:20) for 2 h at 37°C. The dual-labeled sections were contrasted with uranyl acetate and examined under TEM. Control samples were processed separately by incubating with normal rabbit and mouse sera or by omitting primary immunoprobes.

Morphometric analysis was done in images captured at magnification 11,000× from six grids of three independent experiments for nNOS or iNOS in cytoplasm and nucleus [33]. Two gold particles positioned adjacent to each other were also scored.

Statistical analysis

Results are mean ± SEM of at least three to five independent experiments. Comparisons between two groups were performed by unpaired *t*-test with significance at $P < 0.05$.

RESULTS

NO generation, NOS activity, and NOS molecular characteristics evaluation in rat PMNs

NO formation assessment by DAF fluorescence

NO production in the subcellular compartments of PMNs was visualized under a confocal microscope by using DAF-2DA. Fluorescence of DAF was prominently seen in the granules, cytoplasm, and perinuclear region (**Fig. 1B**). It is interesting that it was also evident in the nuclear lobes (Fig. 1B). NO generation in the nucleus suggests a possibility of functional NOS enzyme in the nucleus of PMNs. Arrowheads in Figure 1B indicate the regions of cytoplasm and nucleus with marked DAF fluorescence.

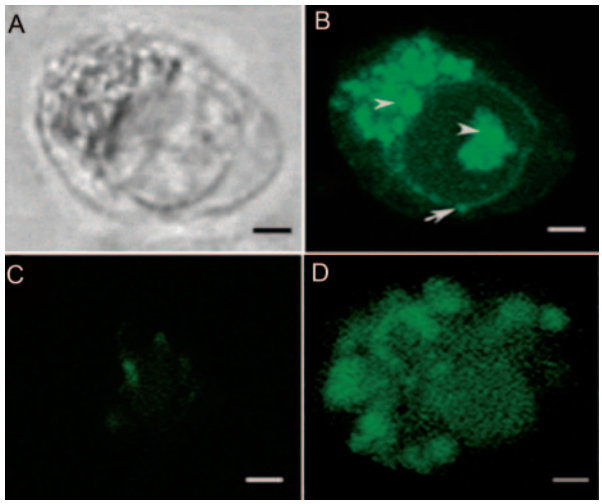

Fig. 1. DAF fluorescence indicating NO production in subcellular compartments of PMNs. (A) Phase micrograph. (B) DAF fluorescence in the same cell (A). Arrowheads demonstrate fluorescence in the nucleus, cytoplasm, and perinuclear region (arrow). (C) DAF fluorescence in 7-NI (1 mM)-pretreated cells. (D) Punctate pattern of fluorescence in the granules and perinuclear region was diffused completely within 20–30 min. The displayed images are representative of five independent experiments. Original bars represent 5 μm (A–D).

Paraformaldehyde fixation of cells prior to the addition of DAF-2DA blocked NO signal. The enzymatic production of NO was also confirmed by the use of NOS inhibitor 7-NI or NOS substrate L-arginine, which were decreased substantially (Fig. 1C) or increased (not shown), respectively. Fluorescent images of DAF-2DA-loaded cells were collected over a period of 5–30 min, the punctate pattern of fluorescence seen in the granules, and nuclear membrane was diffused completely within 20–30 min (Fig. 1D).

Conversion of L-[^{3}H] arginine to L-[^{3}H] citrulline

Direct evidence for the presence of NOS in the NF was obtained by measuring the enzyme activity using L-[^{3}H] arginine. Purity of NFs was ascertained by estimating DNA content and LDH activity. NF exhibited enrichment of DNA content (94%) and negligible LDH activity, and 94% of total LDH activity was found in the CF with DNA below the measurable limit. Purity of the NF was also assessed by electron microscopy, and electron micrographs of a typical PMN have been shown in **Figure 2Ai**. Isolated nuclei of the PMNs are clearly visible with negligible contamination of the cytoplasmic contents (Fig. 2Aii).

Calcium-dependent NOS activity was found only in the CF, and it could not be detected in the NF using defined experimental conditions. Calcium-independent (1 mM EGTA without $CaCl_2$) activity was, however, measurable in nuclear and CFs (Fig. 2C).

NO measurement by flow cytometry

NO generation by DAF-2DA was also measured by flow cytometry in the PMNs and isolated nuclei in the presence of L-arginine (1 mM, NOS substrate) or 7-NI (1 mM, NOS inhibitor). NO formation was augmented in the presence of L-arginine (Fig. 2Bi), and pretreatment of cells with 7-NI signif-

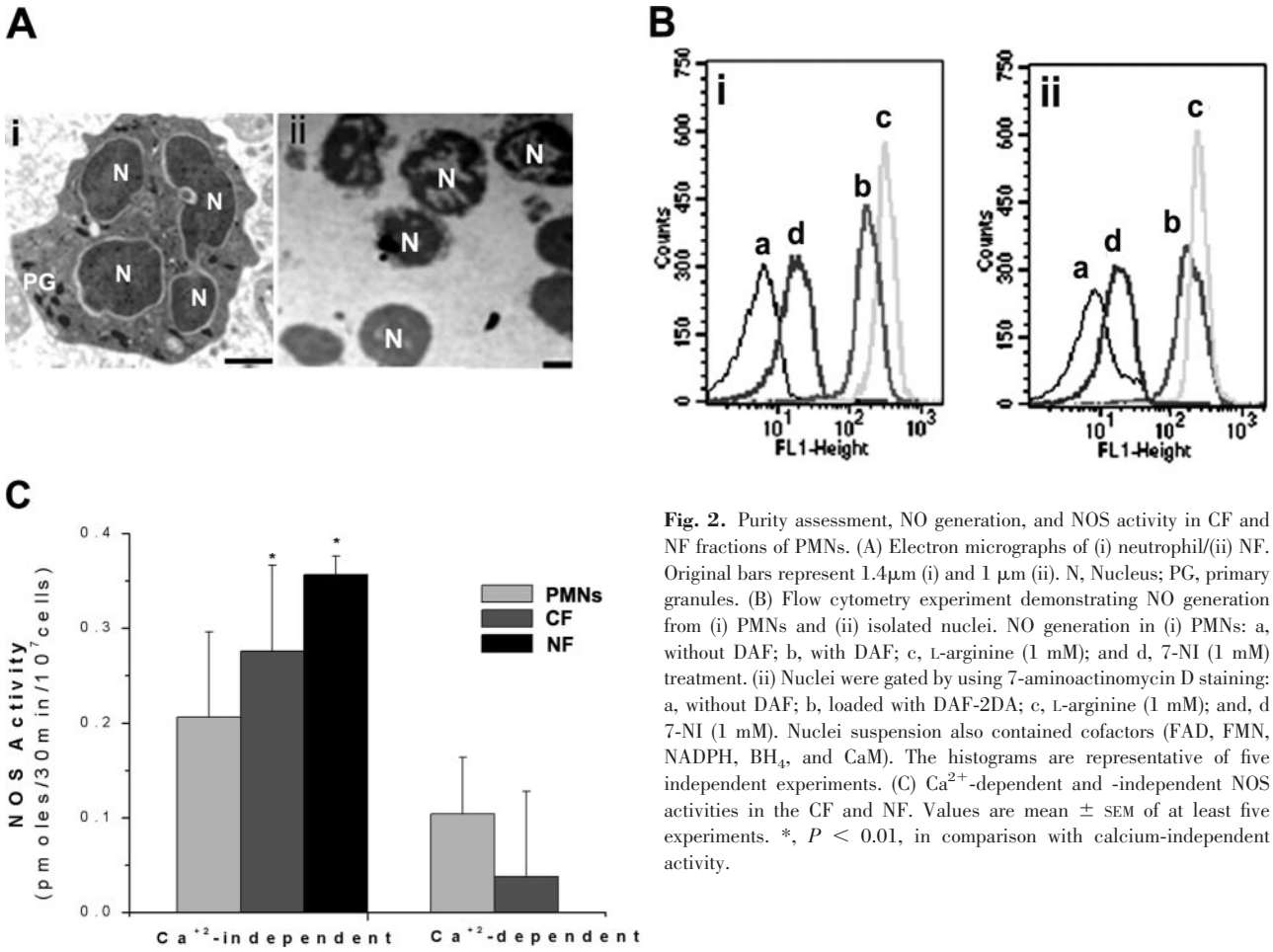

Fig. 2. Purity assessment, NO generation, and NOS activity in CF and NF fractions of PMNs. (A) Electron micrographs of (i) neutrophil/(ii) NF. Original bars represent 1.4μm (i) and 1 μm (ii). N, Nucleus; PG, primary granules. (B) Flow cytometry experiment demonstrating NO generation from (i) PMNs and (ii) isolated nuclei. NO generation in (i) PMNs: a, without DAF; b, with DAF; c, L-arginine (1 mM); and d, 7-NI (1 mM) treatment. (ii) Nuclei were gated by using 7-aminoactinomycin D staining: a, without DAF; b, loaded with DAF-2DA; c, L-arginine (1 mM); and, d 7-NI (1 mM). Nuclei suspension also contained cofactors (FAD, FMN, NADPH, BH_4, and CaM). The histograms are representative of five independent experiments. (C) Ca^{2+}-dependent and -independent NOS activities in the CF and NF. Values are mean ± SEM of at least five experiments. *, $P < 0.01$, in comparison with calcium-independent activity.

icantly reduced NO generation. Similar assay in the NF of PMNs also demonstrated an increase in NO synthesis in the presence of NOS substrate, L-arginine, and attenuation in the presence of NOS inhibitor 7-NI (Fig. 2Bii). It confirmed NOS-dependent NO synthesis in the NF.

Molecular characterization of NOS

To identify NOS isoforms in the PMNs, RT-PCR experiments were conducted by isolating RNA. The presence of nNOS and iNOS was evident (**Fig. 3B**), and signal for eNOS was not detected in the rat PMNs (Fig. 3D). Absence of eNOS (Fig. 3D) and presence of nNOS in PMNs were confirmed by using rat brain as a positive control, and for iNOS, LPS-treated brain was used as a positive control. WB experiments further confirmed the presence of these isoforms in the PMN lysate (Fig. 3, A and C). Level of nNOS expression in PMNs was low in comparison with the cerebellum. Primers used for nNOS detection indicated the presence of the PDZ domain in NOS, which was further substantiated by WB using N-terminal nNOS antibody (K-20: sc-1025).

NOS subcellular localization by immunocytochemistry

Electron microscopy

Exploration of NOS localization by immunoelectron microscopy revealed the presence of nNOS and iNOS in various subcellular compartments in the PMNs. Experiments conducted with mAb as well as polyclonal antibodies (data not shown) exhibited specific labeling and indicated the presence

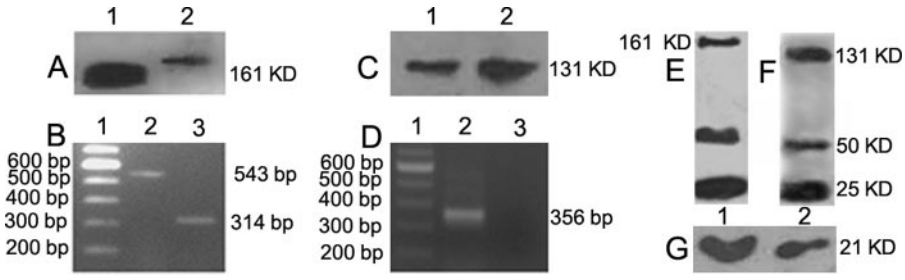

Fig. 3. Molecular characteristics of NOS in rat PMNs. WB of (A) nNOS: lane 1, rat cerebellum (20 μg); lane 2, PMNs (60 μg); (C) iNOS: lane 1, 60 μg; lane 2, 100 μg PMN lysate; and (G) caveolin-1: lane 1, PMN lysate (60 μg); lane 2, fibroblast L929 (60 μg). (B) RT-PCR products of NOS isozymes in rat PMNs. Lane 1, Molecular weight marker; lane 2, nNOS (20 μl); lane 3, iNOS (10 μl). (D) RT-PCR product of eNOS. Lane 1, Molecular weight marker; lane 2, eNOS in rat brain; lane 3, eNOS in rat PMNs. (E) Lane 1, nNOS (20 μl); (F) iNOS (20 μl) in caveolin-1 IP from PMN lysate.

of nNOS as well as iNOS isoforms at various locations. No appreciable binding was seen in the case of labeling only with secondary antibody with variable sizes of gold particles (10 and 15 nm). Evaluation with 5 nm gold particles was, however, obscure or difficult to differentiate from electron-dense granules scattered in the cytoplasm and heterochromatin region of nuclear lobes. Experiments were therefore conducted with 10 and 15 nm gold particles; it was found that immunolabeling with 15 nm gold particles was distinct and more convenient for morphometric analysis.

iNOS and nNOS staining was clearly seen in the nuclear membrane, nucleus (**Figs. 4, B** and **C**, and **5D**) and nuclear pore. iNOS/nNOS immunostaining was quite prominent along the plasma membrane (Figs. 4B and 5C) and in primary granules (Figs. 4D and 5E). The higher magnification clearly showed gold particles corresponding to iNOS in the phagocytic cup (Fig. 4E), cytosol, and mitochondria (Fig. 4F). Comparisons between nNOS and iNOS immunolabeling patterns revealed that nNOS was mostly localized in the cytoplasm, and nNOS immunoreactivity in the nucleus was significantly less than iNOS. Negligible background labeling with no apparent staining in the primary granules, cytoplasm, and nucleus was observed in the controls (Figs. 4A and 5A).

NOS immunolabeling was quite evident as dimers (Figs. 4B and 5B), and in many fields, it was in monomeric form. We counted the gold particles to represent nNOS and iNOS distribution in 15 and 16 representative cells, respectively. Total number of gold particles to represent iNOS distribution in PMNs was 86 ± 5 (n=16), which was significantly more than nNOS (39±2, n=15, $P<0.001$). Among the isoforms, distribution of nNOS was, however, different than iNOS. nNOS was much more in the cytoplasmic compartments (almost 70%), and more than 50% iNOS was localized in the nuclear compartment. Moreover, distribution of iNOS (4±1/cell) and nNOS

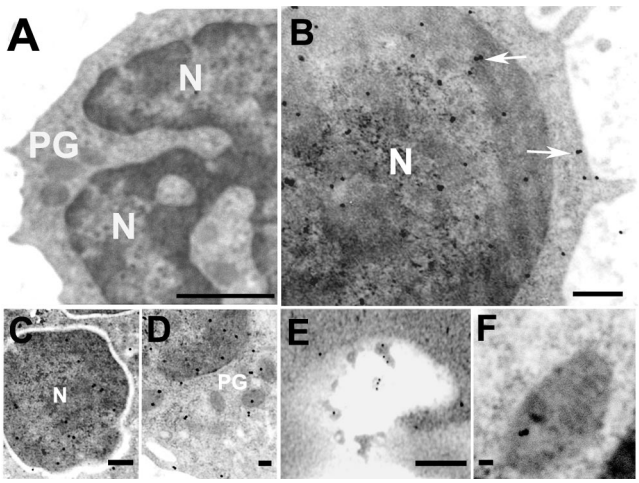

Fig. 4. Localization of NOS in PMNs by immunoelectron microscopy. The presence of iNOS (15 nm) in the nucleus, PG (azurophilic), plasma membrane, nuclear membrane, and cytosol is shown. (A) Immunoreactivity with preimmunized sera was not detected in the control samples. (B) iNOS staining as monomers and dimers (arrows). (C) iNOS in nucleus, (D) in PG, (E) in phagocytic cup (5 nm gold particles), and (F) in mitochondria. Original brs represent 100 mm (A), 0.5 μm (B), 200 nm (C), 20 mm (D), 2 μm (E), and 40 nm (F).

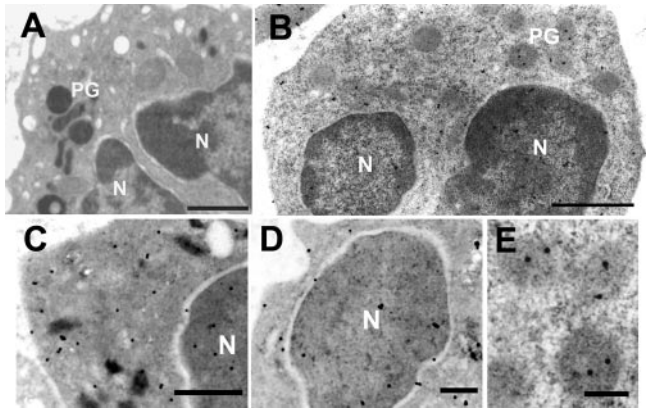

Fig. 5. Distribution of nNOS in the rat PMNs. nNOS is prominently observed in cytoplasm, plasma membrane, nucleus, and nuclear membrane, along the plasma membrane and in primary granules. nNOS staining in (A) negative control treated only with gold-labeled, secondary antibody; (B) cytoplasm, plasma membrane, nucleus, and nuclear membrane; (C) along the plasma membrane; (D) nucleus and nuclear membrane; and (E) primary granuels. Original bars represent 500 nm (A), 1 μm (B), and 200 nm (C–E).

(5±2/cell) was similar in the azurophilic granules, and association of nNOS (15±1/cell) with the plasma membrane was significantly higher than iNOS (8±2/cell, $P<0.005$).

Confocal microscopy

The presence of iNOS and nNOS in nuclear lobes of PMNs was further assessed by immunofluorescent microscopy, which visualized many cells to provide more information in the same experiment. iNOS and nNOS showed plasmalemmal, cytoplasmic, as well as nuclear distribution. Three main sites could be visualized clearly in these acquisitions. First, most of the cells showed diffused intracytoplasmic staining, although nNOS staining intensity showed less variability, but iNOS staining differed in intensity from cell to cell. Second, we found staining in a discrete intracellular punctate pattern (**Fig. 6, Aii** and **Bii**), consistent with a granular/vacuolar localization of NOS. Third, staining was clearly visible in the nuclear lobes but was less than the cytoplasm (Fig. 6, Aii and Bii), which could be a result of the less approachability of antibody in the nuclear lobes, as binding was done in permeabilized cells, unlike sections being used for electron microscopy. To determine whether nNOS and iNOS were localized within the nucleus, we stained nucleus as well as cells with NOS antibodies. Figure 6, Aii and Bii, provided convincing evidence of nNOS (red) and iNOS (red) in the nuclear lobes (as shown by arrowheads) of PMNs. Preimmunized, serum-related immunoreactivity was not detected in negative control samples (Fig. 6, Av and Bv).

IP and identification of NOS-interacting protein

As nNOS and iNOS interact with several proteins in various cells, we explored the possibility of NOS interaction with caveolin-1, an important NOS-interacting protein. We used caveolin-1 antibody for IP; following SDS-PAGE, the blots were probed with nNOS or iNOS antibody. The presence of both NOS isoforms was seen (Fig. 3, E and F), thus suggesting interaction of nNOS and iNOS with caveolin-1. The presence of caveolin-1 in PMN lysate was also evident by WB (Fig. 3G).

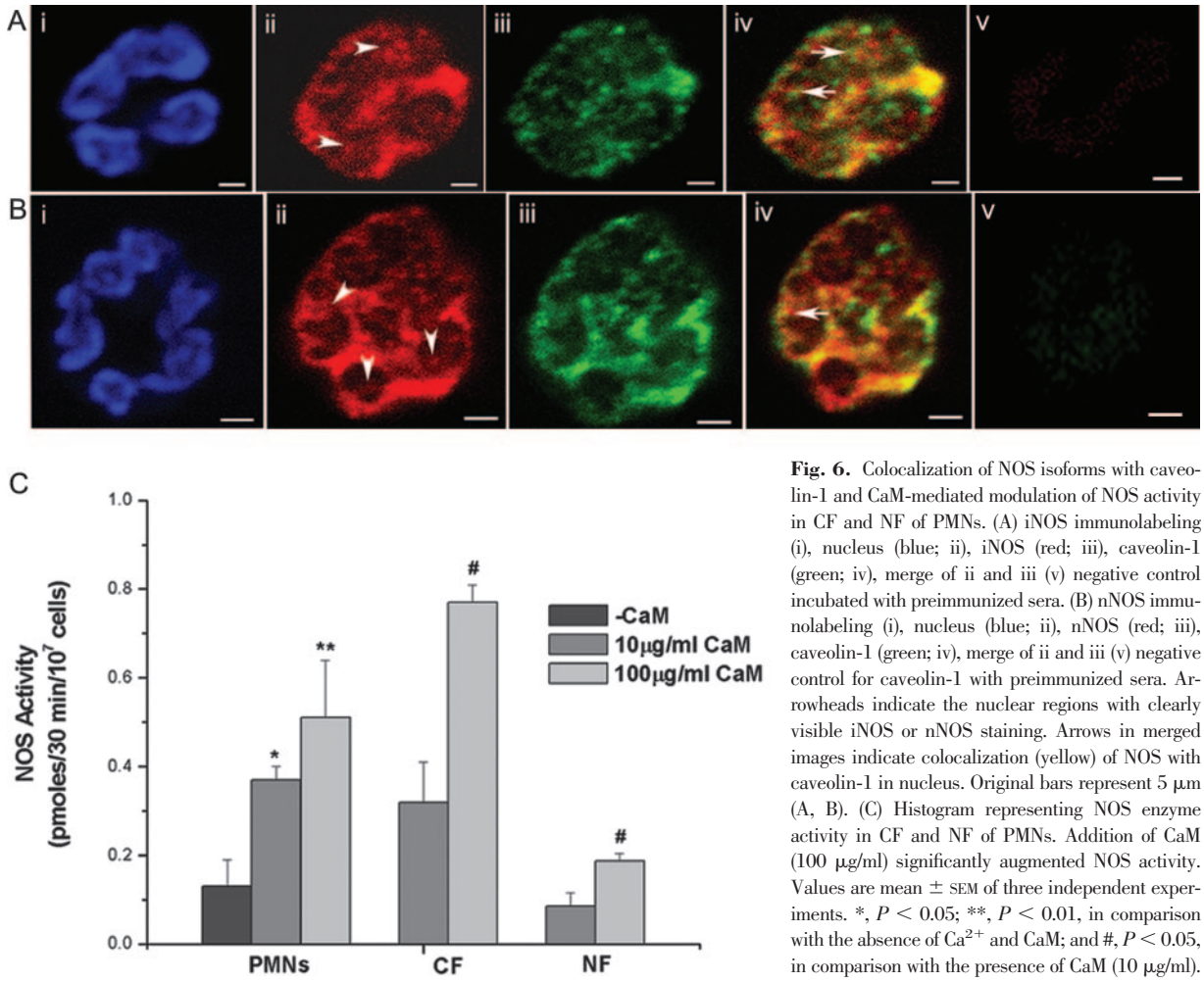

Fig. 6. Colocalization of NOS isoforms with caveolin-1 and CaM-mediated modulation of NOS activity in CF and NF of PMNs. (A) iNOS immunolabeling (i), nucleus (blue; ii), iNOS (red; iii), caveolin-1 (green; iv), merge of ii and iii (v) negative control incubated with preimmunized sera. (B) nNOS immunolabeling (i), nucleus (blue; ii), nNOS (red; iii), caveolin-1 (green; iv), merge of ii and iii (v) negative control for caveolin-1 with preimmunized sera. Arrowheads indicate the nuclear regions with clearly visible iNOS or nNOS staining. Arrows in merged images indicate colocalization (yellow) of NOS with caveolin-1 in nucleus. Original bars represent 5 μm (A, B). (C) Histogram representing NOS enzyme activity in CF and NF of PMNs. Addition of CaM (100 μg/ml) significantly augmented NOS activity. Values are mean ± SEM of three independent experiments. *, $P < 0.05$; **, $P < 0.01$, in comparison with the absence of Ca^{2+} and CaM; and #, $P < 0.05$, in comparison with the presence of CaM (10 μg/ml).

NOS and caveolin-1 colocalization studies

To investigate iNOS and nNOS colocalization with caveolin-1 in the PMNs, we used immunoelectron microscopy as well as confocal immunofluorescence microscopy. Colocalization of iNOS and nNOS with caveolin-1 was performed by using 15 nm gold-conjugated secondary antibodies to immunolabel iNOS or nNOS and 10 nm gold-conjugated secondary antibodies to label caveolin-1, which was mostly found as oligomers (**Fig. 7, A** and **B**) as clusters of two to four gold particles corresponding to caveolin-1, which were occasionally present adjacent to the plasma membrane, nuclear membrane, nucleus, and cytoplasm. iNOS (15 nm gold particle) colocalization with caveolin-1 (10 nm gold particles) is seen in the cytoplasm (Fig. 7D) and inside the nucleus (Fig. 7C). As nNOS immunostaining was always less as compared with iNOS, areas of colocalization of nNOS with caveolin-1 were also relatively less in the cytoplasmic and nuclear compartments. Single labeling was also done simultaneously with double-labeling experiments for caveolin-1 and NOS by using 10 and 15 nm, respectively, to ascertain any artifactually cross-labeling.

To further corroborate these findings, iNOS/nNOS colocalization with caveolin-1 was also evaluated by confocal microscopy. In these experiments, OG 488-labeled secondary antibody was used, as density of NOS or caveolin-1 was not high in these cells. No fluorescence was observed when the cells were incubated alone with the secondary antibody. Caveolin-1 antibody binding was quite marked as was immunofluorescence labeling of iNOS (Fig. 6Aii) or nNOS (Fig. 6Bii). NOS and caveolin-1 exhibited subcellular distribution in cytoplasm as well as in the nucleus. A punctate pattern of fluorescence was seen in the plasmalemma and cytoplasm with relatively less staining of NOS and caveolin-1 in the nucleus (Fig. 6, A and B). Nuclear distribution of caveolin-1 was more in comparison with NOS isoforms (Fig. 6, Aiii and Biii). Areas of colocalization (Fig. 6, Aiv and Biv) of the two proteins are clearly evident as yellow in the merged images.

CaM-mediated modulation of NOS activity

NOS activity in the PMN lysates NF and CF was estimated in the absence and presence of CaM (10 and 100 μg/ml; Fig. 6C). With a tenfold increase in CaM concentration, NOS activity was augmented significantly in the nuclear (117%) as well as in the CFs (140%; Fig. 6C), indicating possible activity modulation of NOS by caveolin-1 and CaM in the PMNs.

DISCUSSION

Intracellular messengers, including pleiotrophic molecule NO, modulate diverse signaling cascades in the various subcellular

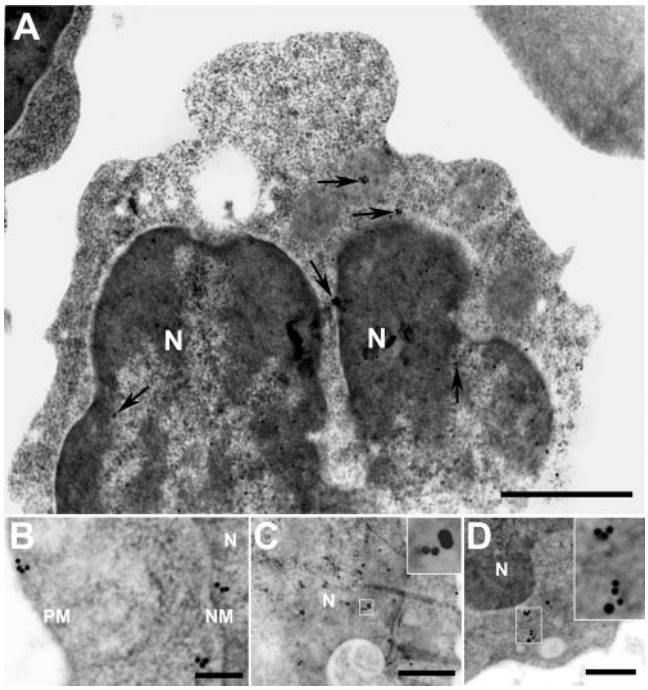

Fig. 7. Colocalization of NOS with caveolin-1 in rat PMNs. (A) Caveolin-1 (10 nm) localization in rat PMNs by immunoelectron microscopy. Arrows indicate clearly visible caveolin-1 immunolabeling. (B) Caveolin-1 immunolabeling (oligomers) prominently seen in the nucleus, nuclear membrane (NM), and plasma membrane (PM). (C) Colocalization of iNOS (15 nm) with caveolin-1 (10 nm) in the nucleus and (D) cytoplasm. Areas of colocalization shown are magnified in insets. Original bars represent 100 nm (A) and 100 mm (B–D).

compartments to regulate PMN functions such as adhesion, chemotaxis, phagocytosis, respiratory burst, and apoptosis. NOS inhibition augmented the number of neutrophils in the mouse bone marrow and blood, suggesting a regulatory role of NO, even in hematopoiesis [34]. Specific functions of NO in neurons, skeletal muscles, and endothelial cells have been attributed to NOS localization in a particular compartment, despite that NO can easily reach to distant targets by diffusion [25, 35, 36]. Such compartmentalized distribution of NOS has not yet been explored in the PMNs. The present study aims to investigate intracellular NOS expression in rat-circulating PMNs by using a combination of biochemical, molecular, confocal, and immunoelectron microscopy techniques.

The N-nitrosation of DAF, a NO detection dye yielding a highly green fluorescent triazole form (DAF-2T), offers not only the advantages of specificity, sensitivity, and a simple protocol for the direct NO detection but also sufficient resolution to locate NO in the subcellular compartments. The observations recorded within 5–10 min after DAF addition exhibited NO formation in the granules, perinuclear region, cytosol, and nuclear lobes (Fig. 1B), which was significantly reduced in the presence of NOS inhibitor 7-NI (Fig. 1C). Fluorescent images collected after 20–30 min did not show the punctate pattern of fluorescence in the granules and nuclear membrane, rather a completely diffused pattern was seen (Fig. 1D). In view of the NO diffusibility [37], a part of fluorescence in the nucleus could be a result of its dispersion from cytoplasmic compartments. Experiments with DAF were suggestive of NO formation in the subcellular compartments and prompted us to undertake systematic evaluation of NOS localization in the PMNs.

Prior to the NOS distribution studies, molecular characteristics of NOS were verified by RT-PCR using isoform-specific primers. The presence of nNOS and iNOS mRNA in the PMNs was seen (Fig. 3B), and eNOS mRNA could not be detected (Fig. 3D). nNOS and iNOS expression was further confirmed by WB (Fig. 3, A and C). Only one report was found in literature about the characterization of NOS isoforms in rat PMNs [14]. The level of nNOS expression in PMNs was low in comparison with the cerebellum, which is in agreement with our finding [14]. Constitutive expression of iNOS in the present study was, though, surprising, as iNOS induction was observed by Greenberg et al. [14] within 2 h after LPS treatment or bacterial infections, with no adverse effect on the nNOS expression. We had also observed a significant increase in NOS activity in PMNs after LPS treatment in rats [5]. Ambient bacterial load could be responsible for the constitutive presence of iNOS in the present study. Controversy in the expression of NOS isoforms in rat brain has also been documented [38]. A systematic study conducted by Keilhoff et al. [38] demonstrated detectable mRNA for iNOS and nNOS in rat brain during embryonic development on Day 10, and proteins were detected only at Day 15; others, however, failed to observe a constitutive presence of iNOS in rat brain. Human PMNs, which exhibit similar functional responses to the addition of NO donors [1], however, constitutively express nNOS and iNOS [14, 39]. Constitutive presence of iNOS has been documented in some cells and is not considered to be the only inducible activity [40]. PMNs, an important part of innate immunity, offer protection against microbes due to generation of reactive oxygen and nitrogen species. Constitutive expression of iNOS in PMNs is to support NO synthesis in large amounts, and macrophages express iNOS only after exposure to LPS [40].

Based on WB and RT-PCR experiments (Fig. 3, A and B), nNOS in rat PMNs seems to be a full-length PDZ domain-containing protein [15]. PDZ domains are protein-interaction domains, which play an important role in the targeting of proteins to specific membrane compartments and their assembly into supramolecular complexes. PDZ domains, though, share a common, three-dimensional structure but generally, differ in their binding specificities. PDZ proteins mostly interact with target proteins without disrupting the overall structure and ligand function as a result of their ability to bind short, extreme C-terminal sequences [41–43]. PDZ domain interaction with the carboxyterminal tail is critical for PSD-95, K+ channels, and the *N*-methyl-D-aspartate receptor clustering, suggesting the physiological relevance of proper subcellular localization of these proteins [23]. PDZ domain of syntrophin mediates association of nNOS with the dystrophin complex in the skeletal muscles [35]. Receptor tyrosine phosphatase-like protein, phosphofructokinase, calcium/CaM-dependent ATPase, and carboxy-terminal-binding protein [41, 42, 44] are also some important PDZ-interacting proteins. The last two proteins have a strong presence in the nuclear compartment and regulate transcription. As nNOS in PMNs also possess a PDZ domain, it is likely to interact with PDZ domain-interacting proteins in PMNs to regulate some important functions. The

results obtained thus warrant further investigations to identify the NOS-interacting proteins in PMNs.

Distribution of nNOS and iNOS proteins was subsequently explored in the fixed PMNs by confocal and immunoelectron microscopy. Differences in the expression of nNOS and iNOS with distinct overlapping in their distribution in various intracellular compartments [azurophilic granules (Figs. 4D and 5E), mitochondria (Fig. 4F), endoplasmic reticulum (not shown), and phagocytic vacuoles (Fig. 4E)] and their prominent presence in nucleus were evidenced (Figs. 4–6). NOS colocalization was documented with myeloperoxidase within primary granules [2], which was also apparent in the present study (Figs. 4D and 5E). The presence of NOS in various subcellular compartments such as mitochondria [45], cardiac sarcoplasmic reticulum [46], insulin secretary granules [47], and mast cell granules [48] has been documented. Moreover, the presence of NOS isoforms in the nucleus of the cultured neonatal cardiomyocytes [46], pancreatic β-cells [47], brown adipocytes [10], mast cells [48], and astrocytes [11] has also been reported. NOS distribution in the subcellular compartments might be to restrict NO signaling to specific sites to perform explicit functions. To delineate the significance of nuclear NOS in PMNs, its role/trafficking in the myeloid cell lineage with particular emphasis on neutrophil maturation should be investigated.

Moreover, studies about NOS in the nuclear compartment demonstrated distinct patterns. In the cultured astrocytes, nNOS translocation to the nucleus on seventh day lasted for only 10 h, which was speculated to down-regulate iNOS transcription [11]. Augmentation in the intracellular calcium level during mast cell activation further enhanced eNOS translocation to the nucleus, but nNOS distribution remained unaltered [48]. All the studies conducted so far have remained speculative to define the role of nuclear NOS [10, 11, 46–48]. Besides, nuclear localization of CaM [49] and BH_4 biosynthetic enzymes [12] are of significant relevance to the presence of NOS in this compartment. S-Nitrosylated glyceraldehyde 3-phosphate dehydrogenase has been found to initiate apoptotic cell death in neurons, indicating that S-nitrosylation is a ubiquitous, post-translational modification to regulate protein functions and their translocation [50]. NO-mediated S-nitrosylation, ubiquitination, oxidation, protein phosphorylation, activation of phosphatases, or altered protein interactions might activate or inhibit transcription by modulating transcription factors and signaling cascade [51, 52]. Even initiation of the transcription process by RNA polymerase I and II in conjunction with actin and myosin I [53] seems to be modulated by cyclic guanosine 3′,5′-monophosphate-dependent protein kinase by dephosphorylating myosin light chain [54], which further signifies the presence of intranuclear NOS. Studies are, however, required to define the exact role of NOS/NO in the nuclear compartment.

Morphometric analysis of the cells after immunoelectron microscopy revealed that PMNs have more iNOS in comparison with nNOS, which is in agreement with the biochemical assessment of NOS activity (Figs. 1 and 2C). iNOS immunoreactivity was almost equally distributed in the nucleus and cytoplasm. Although 70% of the total nNOS resided in the cytoplasm (subcellular organelles excluding nucleus), only 30% was localized in the nucleus. Calcium-independent activity, which is possibly a result of iNOS, was found in NF and CF (Fig. 2C), exhibiting good correlation with the morphometric analysis. Although the presence of nNOS was evident in the nucleus by immunolabeling (Figs. 5B and 6Bii), calcium-dependent NOS activity was detected only in the cytoplasm and could not be measured under the experimental conditions used in the NF (Fig. 2C). Kinetic parameters for NO synthesis, such as oxygen affinity and dissociation constant to release NO from heme, are distinctly different for nNOS and iNOS [55]. nNOS is likely to synthesize NO as well as nitrate, and iNOS can sustain NO formation even during hypoxic conditions. As nNOS binding and calcium-dependent NOS activity are mostly enriched in the cytoplasm, its metabolite nitrite and nitrate are likely to be used more effectively in combination with myeloperoxidase and hypochlorous acid to generate toxic nitrogen species, nitryl chloride, and nitrogen dioxide [5, 56, 57]. iNOS, which generate NO, even at low oxygen tension, might have important implications in inflammatory conditions and cell survival. Although unprecedented, based on existing results, it can be extrapolated that NOS might even perform functions other than NO synthesis, such as protein activity modulation by physical interactions, and their localization in the specific cellular compartment may not necessarily require enzymatically active NOS.

A tenfold increase in CaM concentration augmented NOS activity substantially and significantly in both of the compartments (Fig. 6C). CaM, in high concentrations, displaces binding of NOS with negative regulatory proteins, such as caveolin-1 [24]. Moreover, inhibitory influence of the autoinhibitory loop at a FMN-binding site in nNOS is also removed by the excess CaM [58–60]. Although the presence of caveolin-1 in human PMNs is controversial [61, 62], no such report is available about rat PMNs. The present study thus explored the presence of caveolin-1 in the rat PMNs, which down-regulates activity of all three NOS isoforms [25, 26, 63, 64]. Caveolin-1 antibody (Santa Cruz Biotechnolgoy, N-20: sc-894), used by us to demonstrate the presence of the caveolin-1 α isoform (full-length caveolin), has been used frequently by other investigators [64, 65]. Caveolin-1 and its oligomers in rat PMNs were seen by electron microscopy (Fig. 7, A and B) and subsequently confirmed by WB and IP (Fig. 3, E–G). Caveolin-1 IP was positive for nNOS (Fig. 3E) and iNOS (Fig. 3F) when probed with NOS antibodies, indicating their interaction in the rat PMNs. Confocal and electron microscopy also confirmed colocalization of nNOS and iNOS with caveolin-1 (Figs. 6, Aiv and Biv, and 7, C and D). Caveolin-1, apart from keeping the enzyme inhibited in the resting cells, can also help in the trafficking of NOS to different subcellular compartments [9, 66, 67]. Use of caveolin-1 peptides might thus help to delineate mechanisms involved in CaM-induced activation of NOS and identify the specific amino acids responsible for the observed interaction.

The results obtained indicate a constitutive presence of iNOS, nNOS, and caveolin-1 in the subcellular compartments of rat PMNs including nucleus. NOS seems to interact with caveolin-1 in PMNs and remains inhibited. The present study demonstrates for the first time functionally active NOS isoforms in the nuclear and intracellular compartments, adding a new approach to ascertain the significance of NO in diverse functions of PMNs. As the initial product of NOS enzymatic catal-

ysis is a ferric heme-NO complex and not free NO [55], localization of NOS in subcellular compartments of rat PMNs may serve a definitive role in the compartmentalized redox signaling.

ACKNOWLEDGMENTS

The study was supported by a financial grant to M. D. from the Department of Science and Technology, New Delhi, India, and an award of research fellowships to R. Saini, S. P., and R. Saluja from the Council of Scientific and Industrial Research, New Delhi, India. The authors gratefully acknowledge the critical suggestions of Dr. Gopal Pande (Centre for Cellular and Molecular Biology, Hyderabad, India) and the technical help provided by Mrs. Abha Arya, Mrs. Madhuli Srivastava, and Mr. A. L. Vishwakarma.

REFERENCES

1. Sethi, S., Dikshit, M. (2000) Modulation of polymorphonuclear leukocytes function by nitric oxide. *Thromb. Res.* **100,** 223–247.
2. Evans, T. J., Buttery, L. D. K., Carpenter, A., Springall, D. R., Polak, J. M., Cohen, J. (1996) Cytokine-treated human neutrophils contain inducible nitric oxide synthase that produces nitration of ingested bacteria. *Proc. Natl. Acad. Sci. USA* **93,** 9553–9558.
3. Seth, P., Kumari, R., Dikshit, M., Srimal, R. C. (1994) Modulation of rat peripheral polymorphonuclear leukocyte response by nitric oxide and arginine. *Blood* **84,** 2741–2748.
4. Sethi, S., Singh, M. P., Dikshit, M. (1999) Nitric oxide-mediated augmentation of polymorphonuclear free radical generation after hypoxia-reoxygenation. *Blood* **93,** 333–340.
5. Sethi, S., Sharma, P., Dikshit, M. (2001) Nitric oxide and oxygen derived free radical generation from control and lipopolysaccharide-treated rat polymorphonuclear leukocyte. *Nitric Oxide* **5,** 482–493.
6. Sharma, P., Barthwal, M. K., Dikshit, M. (2002) NO synthesis and its regulation in the arachidonic-acid-stimulated rat polymorphonuclear leukocytes. *Nitric Oxide* **7,** 119–126.
7. Sharma, P., Raghavan, S. A. V., Dikshit, M. (2003) Role of ascorbate in the regulation of nitric oxide generation by polymorphonuclear leukocytes. *Biochem. Biophys. Res. Commun.* **309,** 12–17.
8. Sharma, P., Raghavan, S. A. V., Saini, R., Dikshit, M. (2004) Functional role of ascorbic acid in the regulation of free radical generation and phagocytosis by polymorphonuclear leukocytes: a NO-mediated effect. *J. Leukoc. Biol.* **75,** 1070–1078.
9. Feng, Y., Venema, V. J., Venema, R. C., Tsai, N., Caldwell, R. B. (1999) VEGF induces nuclear translocation of Flk-1/KDR, endothelial nitric oxide synthase, and caveolin-1 in vascular endothelial cells. *Biochem. Biophys. Res. Commun.* **256,** 192–197.
10. Giordano, A., Tonello, C., Bulbarelli, A., Cozzi, V., Cinti, S., Carruba, M. O., Nisoli, E. (2002) Evidence for a functional nitric oxide synthase system in brown adipocyte nucleus. *FEBS Lett.* **514,** 135–140.
11. Yuan, Z., Liu, B., Yuan, L., Zhang, Y., Dong, X., Lu, J. (2004) Evidence of nuclear localization of neuronal nitric oxide synthase in cultured astrocytes of rats. *Life Sci.* **74,** 3199–3209.
12. Elzaouk, L., Laufs, S., Heerklotz, D., Leimbacher, W., Blau, N., Resibois, A., Thony, B. (2004) Nuclear localization of tetrahydrobiopterin biosynthetic enzymes. *Biochim. Biophys. Acta* **1670,** 56–68.
13. Yui, Y., Hattori, B., Kosuga, K., Eizawa, H., Hiki, K., Ohkawa, S., Ohinishi, K., Terao, S., Kawai, C. (1991) Calmodulin-independent nitric oxide synthase from rat polymorphonuclear neutrophils. *J. Biol. Chem.* **266,** 3369–3371.
14. Greenberg, S. S., Ouyang, J., Zhao, X., Giles, T. D. (1998) Human and rat neutrophils constitutively express neural nitric oxide synthase mRNA. *Nitric Oxide* **2,** 203–212.
15. Alderton, W. K., Cooper, C. E., Knowles, R. G. (2001) Nitric oxide synthases: structure, function and inhibition. *Biochem. J.* **357,** 593–615.
16. Kone, B. C., Kuncewicz, T., Zhang, W., Yu, Z. Y. (2003) Protein interactions with nitric oxide synthases: controlling the right time, the right place, and the right amount of nitric oxide. *Am. J. Physiol. Renal Physiol.* **285,** F178–F190.
17. Ratovitski, E. A., Alam, M., Quick, R. A., McMillan, A., Bao, C., Kozlovsky, C., Hand, T., Johnson, R., Mains, R., Eipper, B., Lowenstein, C. J. (1999a) Kalirin inhibition of inducible nitric-oxide synthase. *J. Biol. Chem.* **274,** 993–999.
18. Ratovitski, E. A., Bao, C., Quick, R. A., McMillan, A., Kozlovsky, C., Lowenstein, C. J. (1999b) An inducible nitric-oxide synthase (NOS)-associated protein inhibits NOS dimerization and activity. *J. Biol. Chem.* **274,** 30250–30257.
19. Dedio, J., Konig, P., Wohlfart, P., Schroeder, C., Kummer, W., Muller-Esterl, W. (2001) NOSIP, a novel modulator of endothelial nitric oxide synthase activity. *FASEB J.* **15,** 79–89.
20. Zimmermann, K., Opitz, N., Dedio, J., Renne, C., Muller-Ester, W., Oess, S. (2002) NOSTRIN: a protein modulating nitric oxide release and subcellular distribution of endothelial nitric oxide synthase. *Proc. Natl. Acad. Sci. USA* **99,** 17167–17172.
21. McDonald, K. K., Zharikov, S., Block, E. R., Kilberg, M. S. (1997) A caveolar complex between the cationic amino acid transporter 1 and endothelial nitric-oxide synthase may explain the "arginine paradox". *J. Biol. Chem.* **272,** 31213–31216.
22. Sun, J., Liao, J. K. (2002) Functional interaction of endothelial nitric oxide synthase with a voltage-dependent anion channel. *Proc. Natl. Acad. Sci. USA* **99,** 13108–13113.
23. Brenman, J. E., Chao, D. S., Gee, S. H., McGee, A. W., Craven, S. E., Santillano, D. R., Wu, Z., Huang, F., Xia, H., Peters, M. F., Froehner, S. C., Bredt, D. S. (1996) Interaction of nitric oxide synthase with the postsynaptic density protein PSD-95 and α1-syntrophin mediated by PDZ domains. *Cell* **84,** 757–767.
24. Ju, H., Zou, R., Venema, V. J., Venema, R. C. (1997) Direct interaction of endothelial nitric oxide synthase and caveolin-1 inhibits synthase activity. *J. Biol. Chem.* **272,** 18522–18525.
25. Sato, Y., Sagami, I., Shimizu, T. (2004) Identification of caveolin-1 interacting sites in neuronal nitric oxide synthase. *J. Biol. Chem.* **279,** 8827–8836.
26. Felley-Bosco, E., Bender, F., Quest, A. F. G. (2002) Caveolin-1-mediated post-transcriptional regulation of inducible nitric oxide synthase in human colon carcinoma cells. *Biol. Res.* **35,** 169–176.
27. Yazdanbakhsh, M., Eckmann, C. M., Roos, D. (1985) Characterization of the interaction of human eosinophils and neutrophils with opsonized particles. *J. Immunol.* **135,** 1378–1384.
28. Sanghavi, D. M., Thelen, M., Thornberry, N. A., Casciola-Rosen, L., Rosen, A. (1998) Caspase-mediated proteolysis during apoptosis: insights from apoptotic neutrophils. *FEBS Lett.* **422,** 179–184.
29. Burton, K. (1956) A study of the conditions and mechanisms of the diphenylamine reaction for the colorimetric estimation of deoxyribonucleic acid. *Biochem. J.* **62,** 315–323.
30. Berryman, M. A., Rodewald, R. D. (1990) An enhanced method for post-embedding immunocytochemical staining which preserves cell membranes. *J. Histochem. Cytochem.* **38,** 159–170.
31. Qiu, W., Kass, D. A., Hu, Q., Ziegelstein, R. C. (2001) Determination of shear stress-stimulated endothelial NO production assessed in real time by 4,5-diaminofluorescein fluorescence. *Biochem. Biophys. Res. Commun.* **286,** 328–335.
32. Klinger, A., Reimann, F. M., Klinger, M. H. F., Stange, E. F. (1997) Clathrin-mediated endocytosis of high density lipoprotein3 in human intestinal Caco-2 cells. A post-embedding immunocytochemical study. *Biochim. Biophys. Acta* **1345,** 65–70.
33. Rizzo, V., McIntosh, D. P., Oh, P., Schnitzer, J. E. (1998) In situ flow activates endothelial nitric oxide synthase in luminal caveolae of endothelium with rapid caveolin dissociation and calmodulin association. *J. Biol. Chem.* **273,** 34724–34729.
34. Michurina, T., Krasnov, P., Balazs, A., Nakaya, N., Vasilieva, T., Kuzin, B., Khrushcov, N., Mulligan, R. C., Enklolpov, G. (2004) Nitric oxide is a regulator of hematopoietic stem cell activity. *Mol. Ther.* **10,** 241–248.
35. Segalat, L., Grisoni, K., Archer, J., Vargas, C., Bertrand, A., Anderson, J. E. (2005) CAPON expression in skeletal muscle is regulated by position, repair, NOS activity, and dystrophy. *Exp. Cell Res.* **302,** 170–179.
36. Reiner, M., Bloch, W., Addicks, K. (2001) Functional interaction of caveolin-1 and eNOS in myocardial capillary endothelium revealed by immunoelectron microscopy. *J. Histochem. Cytochem.* **49,** 1605–1609.
37. Crane, B. R., Tainer, J. A. (1997) The structure of nitric oxide synthase oxygenase domain and inhibitor complexes. *Science* **278,** 425–431.
38. Keilhoff, G., Seidel, B., Noack, H., Tischmeyer, W., Stanek, D., Wolf, G. (1996) Patterns of nitric oxide synthase at the messenger RNA and protein levels during early rat brain development. *Neuroscience* **75,** 1193–1201.

39. Cedergren, J., Follin, P., Forslund, T., Lindmark, M., Sundqvist, T., Skogh, T. (2003) Inducible nitric oxide synthase (NOS II) is constitutive in human neutrophils. *APMIS* **111,** 963–968.
40. Michel, T., Feron, O. (1997) Perspective series: nitric oxide and nitric oxide synthases. Nitric oxide synthases: which, where, how, and why? *J. Clin. Invest.* **100,** 2146–2152.
41. Firestein, B. L., Bredt, D. S. (1999) Interaction of neuronal nitric oxide synthase and phosphofructokinase-M. *J. Biol. Chem.* **274,** 10545–10550.
42. Riefler, G. M., Firestein, B. L. (2001) Binding of neuronal nitric oxide synthase (nNOS) to carboxy-terminal-binding protein (CtBP) changes the localization of CtBP from nucleus to the cytosol: a novel function for targeting by the PDZ domain of nNOS. *J. Biol. Chem.* **276,** 48262–48268.
43. Ort, T., Maksimova, E., Dirkx, R., Kachinsky, M. M., Berghs, S., Froehner, S. C., Solimena, M. (2000) The receptor tyrosine phosphatase-like protein ICA512 binds the PDZ domains of β2-syntrophin and nNOS in pancreatic β-cells. *Eur. J. Cell Biol.* **79,** 621–630.
44. Schuh, K., Uldrijan, S., Telkamp, M., Rothlein, N., Neyses, L. (2001) The plasma membrane calmodulin-dependent calcium pump: a major regulator of nitric oxide synthase I. *J. Cell Biol.* **155,** 201–205.
45. Gao, S., Chen, J., Brodsky, S. V., Huang, H., Adler, S., Lee, J. H., Dhadwal, N., Cohen-Gould, L., Gross, S. S., Goligorsky, M. S. (2004) Docking of endothelial nitric oxide synthase (eNOS) to the mitochondrial outer membrane. *J. Biol. Chem.* **279,** 15968–15974.
46. Xu, K. Y., Huso, D. L., Dawson, T. M., Bredt, D. S., Becker, L. C. (1999) Nitric oxide synthase in cardiac sarcoplasmic reticulum. *Proc. Natl. Acad. Sci. USA* **96,** 657–662.
47. Lajoix, A. D., Reggio, H., Chardes, T., Peraldi-Roux, S., Tribillac, F., Roye, M., Dietz, S., Broca, C., Manteghetti, M., Ribes, G., Wollheim, C. B., Gross, R. (2001) A neuronal isoform of nitric oxide synthase expressed in pancreatic β-cells controls insulin secretion. *Diabetes* **50,** 1311–1323.
48. Gilchrist, M., McCauley, S. D., Befus, A. D. (2004) Expression, localization, and regulation of NOS in human mast cell lines: effects on leukotriene production. *Blood* **104,** 462–469.
49. Bachs, O., Agell, N., Carafoli, E. (1992) Calcium and calmodulin function in the cell nucleus. *Biochim. Biophys. Acta* **1113,** 259–270.
50. Hara, M. R., Agarwal, N., Kim, S. E., Cascio, M. B., Fujimuro, M., Ozeki, Y., Takahashi, M., Cheah, J. H., Tankou, S. K., Hester, L. D., Ferris, C. D., Hayward, S. D., Snyder, H. S., Sawa, A. (2005) S-Nitrosylated GAPDH initiates apoptotic cell death by nuclear translocation following Siah1 binding. *Nat. Cell Biol.* **7,** 663–674.
51. Turpaev, K., Bouton, C., Diet, A., Glatingny, A., Drapier, J. C. (2005) Analysis of differentially expressed genes in nitric oxide exposed human monocytic cells. *Free Radic. Biol. Med.* **38,** 1392–1400.
52. Hess, D. T., Matsumoto, A., Kim, S., Marshall, H. E., Stamler, J. S. (2005) Protein S-nitrosylation: purview and parameters. *Nat. Rev. Mol. Cell Biol.* **6,** 150–166.
53. Philimonenko, V. V., Zhao, J., Iben, S., Dingova, H., Kysela, K., Kahle, M., Zentgraf, H., Hofmann, W. A., de Lanerolle, P., Hozak, P., Grummt, I. (2004) Nuclear actin and myosin I are required for RNA polymerase I transcription. *Nat. Cell Biol.* **6,** 1165–1172.
54. Surks, H. K., Mochizuki, N., Kasai, Y., Georgescu, S. P., Tang, K. M., Ito, M., Lincoln, T. M., Mendelsohn, M. E. (1999) Regulation of myosin phosphatase by a specific interaction with cGMP-dependent protein kinase Iβ. *Science* **286,** 1583–1587.
55. Stuehr, D. J., Santolini, J., Wang, Z., Wei, C., Adak, S. (2004) Update on mechanism and catalytic regulation in the NO synthases. *J. Biol. Chem.* **279,** 36167–36170.
56. Van der Vliet, A., Eiserich, J. P., Halliwell, B., Cross, C. E. (1997) Formation of reactive nitrogen species during peroxidase-catalyzed oxidation of nitrite. *J. Biol. Chem.* **272,** 7617–7625.
57. Eiserich, J. P., Hristova, M., Cross, C. E., Jones, A. D., Freeman, B. A., Halliwell, B., Van Der Vliet, A. (1998) Formation of nitric oxide-derived inflammatory oxidants by myeloperoxidase in neutrophils. *Nature* **391,** 393–397.
58. Su, Z., Blazing, M. A., Fan, D., George, S. E. (1995) The calmodulin-nitric oxide synthase interaction. Critical role of the calmodulin latch domain in enzyme activation. *J. Biol. Chem.* **270,** 29117–29121.
59. Salerno, J. C., Harris, D., Irizarry, K., Patel, B., Morales, A. J., Smith, S. M. E., Martasek, P., Roman, L. J., Masters, B. S. E., Jones, C. L., Weissman, B. A., Lane, P., Liu, Q., Gross, S. S. (1997) An autoinhibitory control element defines calcium-regulated isoforms of nitric oxide synthase. *J. Biol. Chem.* **272,** 29769–29777.
60. Jones, R. J., Smith, S. M. E., Gao, Y. T., DeMay, B. S., Mann, K. J., Salerno, K. M., Salerno, J. C. (2004) The function of the small insertion in the hinge subdomain in the control of constitutive mammalian nitric oxide synthases. *J. Biol. Chem.* **279,** 36876–36883.
61. Yan, S. R., Fumagalli, L., Berton, G. (1996) Activation of SRc family kinases in human neutrophils. Evidence that p58C-FGR and p53/56LYN redistributed to a Triton X-100-insoluble cytoskeletal fraction, also enriched in caveolar protein caveolin, display an enhanced kinase activity. *FEBS Lett.* **380,** 198–203.
62. Sengelov, H., Voldstedlund, M., Vinten, J., Borregaard, N. (1998) Human neutrophils are devoid of the integral membrane protein caveolin. *J. Leukoc. Biol.* **63,** 563–566.
63. Venema, R. C. (2002) Post-translational mechanisms of endothelial nitric oxide synthase regulation by bradykinin. *Int. Immunopharmacol.* **2,** 1755–1762.
64. Bernatchez, P. N., Bauer, P. M., Yu, J., Prendergast, J. S., He, P., Sessa, W. C. (2005) Dissecting the molecular control of endothelial NO synthase by caveolin-1 using cell-permeable peptides. *Proc. Natl. Acad. Sci. USA* **102,** 761–766.
65. Fujimoto, T., Kogo, H., Nomura, R., Une, T. (2000) Isoforms of caveolin-1 and caveolar structure. *J. Cell Sci.* **113,** 3509–3517.
66. Feron, O., Belhassen, L., Kobzik, L., Smith, T. W., Kelly, R. A., Michel, T. (1996) Endothelial nitric oxide synthase targeting to caveolae. Specific interactions with caveolin isoforms in cardiac myocytes and endothelial cells. *J. Biol. Chem.* **271,** 22810–22814.
67. Shaul, P. W., Smart, E. J., Robinson, L. J., German, Z., Yuhanna, I. S., Ying, Y., Anderson, R. G. W., Michel, T. (1996) Acylation targets endothelial nitric oxide synthase to plasmalemmal caveolae. *J. Biol. Chem.* **271,** 6518–6522.